JOURNAL OF CATALYSIS **168,** 235–244 (1997)
ARTICLE NO. CA971622

Microkinetic Analysis of Ammonia Synthesis Based on Surface Reaction Studies of Iron Catalysts as Compared to Single-Crystal Studies

B. Fastrup

Haldor Topsøe Research Laboratories, Nymøllevej 55, PO Box 213, DK-2800 Lyngby, Denmark

Received March 16, 1995; revised December 3, 1996; accepted January 24, 1997

The main purpose of this paper is to analyze recent nitrogen adsorption and desorption studies of iron-based ammonia synthesis catalysts by Langmuir-type models, to some extent with a linear coverage dependence of the activation energies included. The results are applied to set up a simple microkinetic model for the ammonia synthesis reaction, where due care has been taken to choose the kinetic parameters for the relevant range of coverages. This model is self-consistent in that the predicted coverages are within the range used to determine the input parameters, and the agreement between calculations and experiments is much better than for models based on single-crystal studies. A consequence of the analysis is that chemisorbed atomic nitrogen (N–*) is much more weakly bound at high coverages than is to be expected from low-coverage single-crystal studies. The coverage of N–* is close to 0.5 under synthesis conditions, a result that is in agreement with earlier considerations. The experimentally observed differences in the activity, as well as the pressure dependence of the reaction rate, working with catalysts with and without potassium promoter, can be at least partly explained by a destabilization effect of potassium on N–* or on the hydrogenated species NH–*. The main conclusion is that it is necessary to take surface heterogeneity or adsorbate-adsorbate interactions into account to obtain a model that can compete with the Temkin-type models.

1. INTRODUCTION

The kinetics of ammonia synthesis over industrial iron catalysts is still a subject of discussion despite the fact that it has been studied for most of this century. From an industrial point of view, the extended Temkin–Pyzhev equations (1) are most useful in simulating the ammonia yields under various conditions (2), and hence there is no great technological incentive to make further kinetic studies of ammonia synthesis over the industrial iron catalyst.

In recent decades, however, surface science studies of single-crystal surfaces have been used as a basis for attempts to formulate microkinetic models (3–12). The view that the catalyst surface is dominated by the Fe(111) plane, with a negative apparent activation energy of dissociative chemisorption of nitrogen (4–6, 9, 10), came into conflict with the general experience that chemisorption of nitrogen on iron-based catalysts is a very slow and strongly activated process (8, 12–14). It has been suggested (6) that this discrepancy is caused by oxygen poisoning during the conventional chemisorption studies, since it is well known that at low temperatures the industrial catalysts are extremely sensitive to such poisoning, even at sub-parts per million levels of oxygen; however, the single-crystal studies do not support the hypothesis that small amounts of oxygen should lead to a decrease in the rate of chemisorption of several orders of magnitude. A simple site blocking effect was observed (15, 16). Other possible reasons why low-coverage sticking-coefficient results from single-crystal studies may be inappropriate to catalysts have been discussed thoroughly in Refs. (17, 18).

It is well known with kinetic modeling that there are often many ways to obtain a good fit to a set of experimental data. Such fits definitely do not prove that the mechanism concerned is correct, neither with respect to the values of input parameters, nor with regard to the underlying assumptions in the mechanism itself. As expressed in Ref. (19), "the mapping between mechanism and rate expression is unidirectional." In particular, the use of "45° plots" of calculated versus experimental values of the product concentration at the reactor outlet, to illustrate the success of a model, can be very deceptive. For experimental results close to equilibrium, the agreement will always appear satisfactory, provided only that the model does not seriously underestimate the rate. Due to the strong inhibition of the rate of synthesis by even a small partial pressure of ammonia, the range of conditions for which a reasonable 45° plot can be expected will be quite extensive for iron-based catalysts. As demonstrated recently (2), the calculated rate of ammonia synthesis will always be reasonably correct in the limit where $\theta_N \approx 1$, no matter what rate of dissociative chemisorption of nitrogen is assumed, provided only that the rate of nitrogen desorption is correct. For these reasons, the following treatment focuses mainly on low conversion conditions, where θ_N is significantly lower than 1.

Both old and modern studies of elementary or more complicated surface reactions indicate that the surface of an industrial iron-based catalyst is kinetically heterogeneous.

0021-9517/97 $25.00

Hence the great success over the years of the Temkin-type kinetic model is not surprising. Thus one would definitely not expect perfect agreement starting from a simple Langmuir-type model, yet it is instructive to investigate how closely such a model can describe the physicochemical principles and the synthesis kinetics when due care is taken to choose the appropriate kinetic parameters for the relevant coverages. The same is true, e.g., when elementary chemisorption processes are described by an Arrhenius-type rate constant, even when the coverage dependences are much stronger than the Langmuir factors can explain. This problem is then solved by allowing the activation energy as well as the preexponential factor to vary with coverage, the latter frequently by several orders of magnitude ("strong compensation effects") (20).

Temperature-programmed studies have recently been used (18, 21), to map the nitrogen chemisorption characteristics of guaranteed nonpoisoned catalysts; extreme care was taken to ensure that poisoning was really absent. The conclusion was that the process is slow and activated, in good agreement with the earlier results of Scholten *et al.* (14).

In the present article a discussion is presented on the possible consequences of the above-mentioned results for simple Langmuir-type microkinetic analysis. Examples of various ways to obtain a good fit between model and experiment are presented, and the effects of variations in the input parameters are discussed.

2. GENERAL MODEL

The series of steps considered in the modeling of the ammonia synthesis reaction are as usual (2–12):

$$N_2(g) + * \rightleftarrows N_2{-}* \quad [1]$$

$$N_2{-}* + * \rightleftarrows 2N{-}* \quad [2]$$

$$N{-}* + H{-}* \rightleftarrows NH{-}* + * \quad [3]$$

$$NH{-}* + H{-}* \rightleftarrows NH_2{-}* + * \quad [4]$$

$$NH_2{-}* + H{-}* \rightleftarrows NH_3{-}* + * \quad [5]$$

$$NH_3{-}* \rightleftarrows NH_3(g) + * \quad [6]$$

$$H_2(g) + 2* \rightleftarrows 2H{-}* \quad [7]$$

where $*$ denotes a chemisorption site. Fugacity effects are of negligible importance for the results discussed here. They have been taken into account in all cases where direct comparison with experimental data for NH_3 synthesis is made, but for the computations given below ideal gas behavior has been assumed. The results used in the following all originate from experiments using small catalyst particles (i.e., no significant diffusion limitations) in reactors working under plug-flow conditions (6, 18, 22, 23).

The suggested existence of a molecular precursor to the dissociation of nitrogen is crucial to a fundamental understanding of the physical significance of the concept of negative apparent activation energies (24). However, since it is generally accepted that the coverage of molecular nitrogen is low at synthesis temperatures, and since the molecular precursor has proved difficult to observe (21, 25), steps [1] and [2] are mostly replaced by

$$N_2(g) + 2* \rightleftarrows 2N{-}*. \quad [0]$$

In all the computer simulations we have carried out, it has been suggested that none of the other steps should become slower than the dissociative chemisorption of nitrogen. This means that for steps [3] to [7], only the equilibrium constants are of importance.

3. MODELS BASED ON NONACTIVATED NITROGEN CHEMISORPTION

The rate constants deduced from the single-crystal Fe(111) studies are used as a starting point and the factors A and E_A as given in Ref. (11) are listed in Table 1. These rate constants lead to ammonia synthesis rates of the right order of magnitude for potassium-promoted iron catalysts under industrial conditions (2, 4–6, 9–11). Generally, the agreement between calculated and experimental values of the NH_3 concentration at the reactor outlet was good at conversions higher than half of the equilibrium value, at 1, 150, and 300 atm. The calculated-versus-experimental values plot ("45° plot"), however, displayed a systematically deviating trend, resulting in a slope closer to 2/3 than to 1 (4–6). The deviation over the experimental range amounted to a factor of about 2 of the exit NH_3 concentration. Due to the strong inhibition of the synthesis rate by ammonia, this deviation corresponds to a much larger variation in

TABLE 1

Preexponential Factors (A) and Activation Energies (E_A) for Steps in Ammonia Synthesis from Ref. (11)

	Forward step		Reverse step	
Step[a]	A (s^{-1})	E_A (kJ mol^{-1})	A (s^{-1})	E_A (kJ mol^{-1})
0	58.0 [b]	−14.6	1.32×10^9	155.0
1	2.53×10^6 [b]	0.0	1.87×10^{14}	43.1
2	4.29×10^9	28.5	1.32×10^9	155.0
3	1.83×10^9	81.3	1.15×10^7	23.2
4	1.31×10^{13}	36.4	1.38×10^{12}	0.0
5	3.88×10^{13}	38.7	2.33×10^{13}	0.0
6	3.67×10^{12}	39.2	1.81×10^8 [b]	0.0
7	7.01×10^6 [b]	0.0	3.24×10^{13}	93.8

[a] See text.
[b] s^{-1} atm^{-1}.

the equivalent amount of catalyst, as also pointed out by Bowker (17). Stoltze (6) demonstrated that the addition of a small amount (10 ppm) of water could change the slope to 1. Addition of water also increased the activation energy for the synthesis reaction from 47 to ca. 76 kJ mol^{-1}, which is a more realistic value (22, 23). Later, the activation energy for the dissociative nitrogen sticking coefficient in the model was increased from −15 to +3 kJ mol^{-1} (26), which necessarily increased the activation energy for the synthesis reaction as well. The new model can be considered only a minor revision, however, since the nitrogen chemisorption is still considered approximately nonactivated, and the "45° plot" in Ref. (26) is indistinguishable from the original one (4–6); i.e., the slope is still closer to 2/3 than to 1.

An alternative way of increasing the activation energy for NH_3 synthesis would be to increase the H−∗ binding energy. An example of the results of such a procedure is demonstrated in Fig. 1 and in Table 2, column II. The binding energy of NH−∗ has also been changed, but the main effect comes from H−∗. This demonstrates that it is possible to obtain approximately correct NH_3 yields even for low conversions and negative activation energies for the chemisorption of nitrogen, in contrast to what has been claimed (17); however, it can easily be verified from calculations of the equilibrium coverage versus hydrogen pressure that the heat of hydrogen chemisorption in Table 2, column II, is far too high to be consistent with hydrogen TPD results (27). The reverse approach would be to choose a low heat of chemisorption of hydrogen and then change the activation energy for the N_2 dissociation step. This method is dealt with in Section 5.

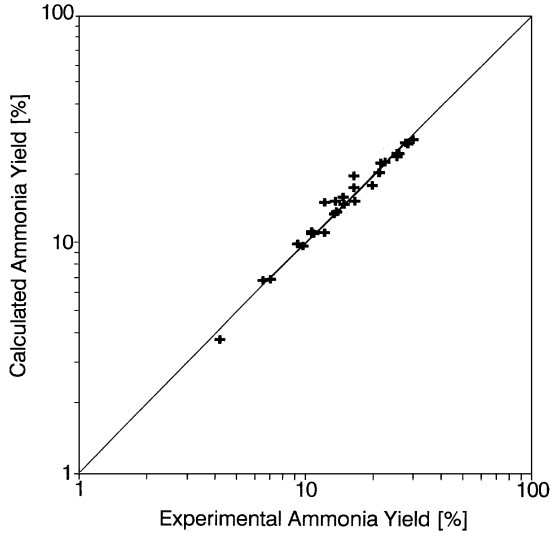

FIG. 1. Calculated versus measured (22, 23) ammonia yields. Case with high heat of chemisorption of hydrogen (Table 2, column II). Multiply promoted catalyst. SV: 15,000–106,000/h, pressure: 150–308 atm, temperature: 646–768 K, NH_3: 4–30%, $H_2:N_2$: 1.2–6.2.

TABLE 2

Reaction Enthalpies at 673 K

	Reaction enthalpy (kJ mol^{-1})	
Step[a]	I[b]	II[c]
0	−169	−169
3	58	100
4	36	30
5	39	50
6	39	44
7	−94	−129

[a] See text.
[b] E_A (forward)−E_A (reverse) from Table 1.
[c] Enthalpies as in column I, but with heat of hydrogen chemisorption increased to fit the activation energy of 76 kJ mol^{-1} for NH_3 synthesis at 150 atm, 723 K, and 8% NH_3.

4. SIMPLE TPD AND TPA MODELING

The following conditions were used in all the modeling work described here: catalyst volume = 0.2 cm^3, gas flow = 50 cm^3/min, pressure = 1 atm. No important effects of plug flow versus constant stirred tank reactor conditions were found. This is self-evident for the TPA but not for the TPD results, as discussed later.

Figure 2 displays the results of calculations of nitrogen TPD profiles using the parameters in Table 1. The position of the nitrogen TPD peak maximum is at ca. 680 K, if the reverse reaction is omitted. This value falls between the experimental values for potassium-promoted and potassium-free samples (650 and 710 K, respectively) (18, 21, 28). The calculations including readsorption are clearly not in

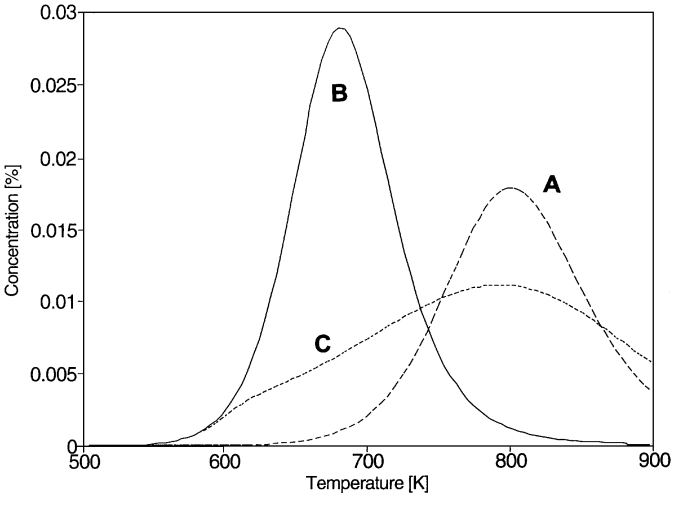

FIG. 2. Calculated N_2 TPD profiles for the rate constants in Table 1. (A) Without readsorption, heating rate: 420 K/min. (B) Without readsorption, heating rate: 5 K/min. (C) Including readsorption, 5 K/min.

agreement with the experiments. Obviously, the calculated rates of readsorption have to be decreased. If an attempt is made to fit both the position and the width of the TPD peak using a low rate of readsorption and a constant preexponential factor A_{-2} ("-2" referring to the reverse step 2) and activation energy E_d, the result will be $A_{-2} \approx 4 \times 10^7\ s^{-1}$ or below and an activation energy $E_d \approx 127$ kJ mol^{-1} is obtained. This does not seem likely. Recent studies of the effects of the chosen heating rate on the TPD peak position (28) suggest that $A_{-2} = 1.3 \times 10^9\ s^{-1}$ is a reasonable value. Fixing this value and fitting the peak position by variation of E_d result in $E_d = 146$ or 163 kJ mol^{-1} for samples with and without potassium, respectively. The resulting TPD peaks are too narrow, basically as shown for the irreversible case in Fig. 2, since the rate constant for desorption is approximately the same; however, only the difference between samples with and without potassium is of concern at this stage. The problem of the peak width is further addressed in Section 7.

The nitrogen TPA reaction is rather complicated to model. This is self-evident from previous results of N_2 chemisorption studies, such as those by Scholten *et al.* (14). Several explanations of the peculiar structure of the TPA peaks can be suggested, as discussed in Ref. (18). Thus, it will be possible to find several solutions to the modeling problem until more data are available. As an example, Table 3 gives some of the solutions to the problem of fitting the high-temperature part of the TPA profile [zones d and e in Ref. (18)], and the corresponding TPA curves are shown in Fig. 3. The number of active sites here and in the following cases have been obtained by fitting the height of the first TPD peak for the sample in question. The preexponential factor 133 s^{-1} atm^{-1} is not too far from the 58 s^{-1} atm^{-1} in Table 1. It is interesting to note that the "bump" [labeled e as in Ref. (18)] just before desorption sets in can (to some extent) be reproduced without introducing another type of site.

A perfect fit of the combined TPA/TPD profiles cannot be obtained within a simple Langmuir model by assuming only one type of site and no coverage dependence of the rate constant. A good fit to the adsorption part results in too sharp a desorption peak. The inadequacy of the Langmuir model is not so surprising since nitrogen chemisorption on iron is the standard textbook example of adsorption with a strongly coverage-dependent enthalpy (Slygin–Temkin isotherm) as well as activation energy (29). In the following section an attempt is made to combine the experience gained with both ammonia synthesis kinetics and elementary surface reactions to investigate how far one can proceed with a Langmuir approach, when due care is taken to choose the kinetic parameters consistently, i.e., for the coverages that will be dominating under the conditions that the model is expected to simulate.

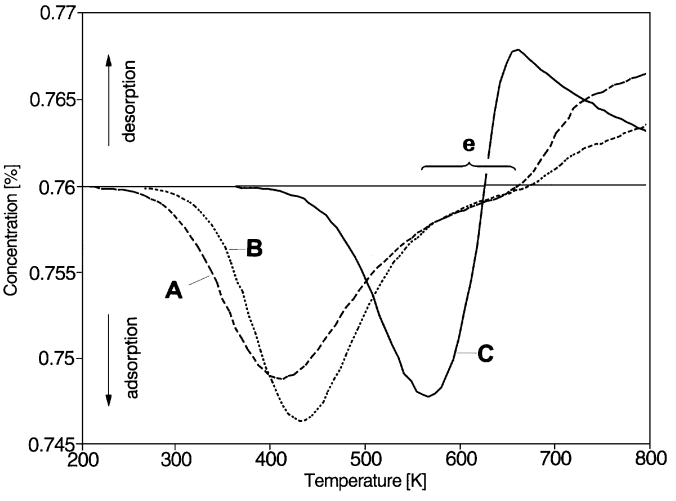

FIG. 3. Calculated TPA profiles for nitrogen. Rate constants and labels from Table 3. Flow: 50 cm^3/min 0.76% N_2 in He, heating rate: 5 K/min, number of active sites: 1.2×10^{19}. e: see text.

TABLE 3

Nitrogen Adsorption and Desorption Rate Parameters Used for Calculation of the TPA Profiles in Fig. 3[a]

Adsorption		Desorption		
A (s^{-1} atm^{-1})	E_{ad} (kJ mol^{-1})	A (s^{-1})	E_d (kJ mol^{-1})	Profile in Fig. 3
133	25.1	5.23×10^8	168	A
1948	35.2	5.23×10^8	173	B
20000	57.6	1.3×10^9	146.3	C

[a] The data in the first two lines were obtained by fitting results for a multiply promoted sample (18).

5. MICROKINETIC ANALYSIS BASED ON CATALYST STUDIES

After thorough reexamination of all the TPA/TPD profiles in Ref. (18) the following approach to a microkinetic model of the ammonia synthesis reaction on potassium-promoted catalysts was attempted.

It was assumed that the relevant active sites are those corresponding to the first peak in the TPD profiles. This was where the most striking difference was found for samples with and without potassium. In addition, the total coverage of N–∗ is expected to be high under synthesis conditions, so the number of free sites on which the reaction can proceed will be significant only for the sites that bind N–∗ most weakly, i.e., the sites giving rise to the first peak. Consequently, the other sites can be ignored as a first approach. The preexponential factor and activation energy for desorption of N_2 were chosen to be $1.3 \times 10^9\ s^{-1}$ and 146.3 kJ mol^{-1}, respectively (cf. Section 4 above). The rate constant for adsorption was then fitted to agreement with the isobars

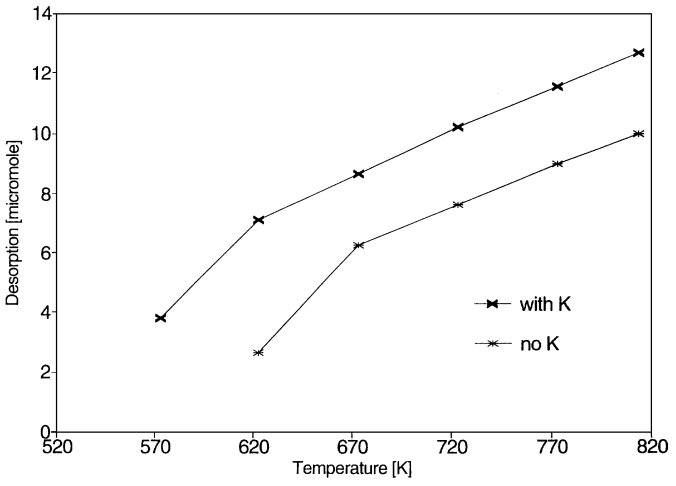

FIG. 4. Nitrogen desorption equilibrium isobars for singly and doubly promoted samples. Partial pressure of N_2: 0.0015 atm.

at about half-coverage (Fig. 4) with due respect to the TPA. The isobars were given priority over the TPA, since the interpretation of the latter is rather complicated. The result (Table 4) is illustrated in Fig. 3. The TPA (solid line) was not in disagreement with experimental results for high coverages, as will be demonstrated later (Fig. 9). It can be noted that the energetics of the nitrogen chemisorption in Table 4 are similar to those suggested in Refs. (17, 30). Results of determinations of the heat of chemisorption of nitrogen (Q) on iron range from 46 to 210 kJ mol^{-1} (12, 31). Obviously, more work on guaranteed nonpoisoned catalysts with various promoters is needed; in particular, direct calorimetric studies would be useful.

The heat of chemisorption of hydrogen was chosen to fit the 300-Torr isobar obtained by conventional hydrogen chemisorption methods for a commercial catalyst [KM1, Fig. 4A in Ref. (32)].

The resulting rate constants (expressed as A and E_A values) for steps [0] and [7] are given in Table 4. The other rate constants have been adjusted to physically "reasonable" values consistent with the gas-phase equilibrium constant [see, for instance, Eq. 3.38 in Ref. (6)]. Step [3] is left almost as in Table 1 and mainly the rate constants for the uncritical steps [4] to [6] have been varied. No fitting was involved for steps [3] to [6]. The resulting 45° plot (21) can hardly be distinguished from the plot in Fig. 1.

An indication of the balance between the equilibrium constants for chemisorption of hydrogen and nitrogen can be obtained from experiments where the $H_2:N_2$ ratio is changed. Figure 5 demonstrates that the present model reproduces this variation almost perfectly, whereas the model relating to the data in Table 1 does not display the initial increase in NH_3 concentration, which has also been reported previously (22). For comparison, the number of active sites was fitted at 50% N_2. Concerning the order of magnitude, it suffices to say that for the data in Fig. 5, both models were in agreement with the expectations, considering the experimental uncertainties and the overall shortcomings of the models.

The rate constants given by the data in Table 4 have the following interesting property. If the heat of chemisorption Q and the activation energy for adsorption and desorption are varied according to the Evans–Polanyi relation,

$$\delta E_a = \alpha \cdot \delta Q, \qquad [8]$$

using $\alpha = 0.75$ (α being the parameter in the Temkin–Pyzhev equation [1]), the result emerges that the rate of NH_3 synthesis is close to optimal. The maximum values for 50% conversion and 673 K are found by decreasing or increasing Q by only ca. 4 kJ mol^{-1} for 100 and 1 atm, respectively.

TABLE 4

Kinetic Parameters (A and E_A) Deduced from Studies of Adsorption and Desorption of Nitrogen and Hydrogen for Potassium-Promoted Fused Iron Oxide Catalysts

	Forward step		Reverse step	
Step[a]	A (s^{-1})	E_A (kJ mol^{-1})	A (s^{-1})	E_A (kJ mol^{-1})
0	2.00×10^{4} [b]	57.60	1.30×10^{9}	146.3
3	1.83×10^{9}	83.60	2.36×10^{7}	20.9
4	1.20×10^{13}	13.38	1.00×10^{13}	0.0
5	1.18×10^{13}	14.63	1.00×10^{13}	0.0
6	4.08×10^{12}	12.54	1.81×10^{8} [b]	0.0
7	7.01×10^{6} [b]	0.00	3.03×10^{13}	74.82

[a] See text.
[b] s^{-1} atm^{-1}.

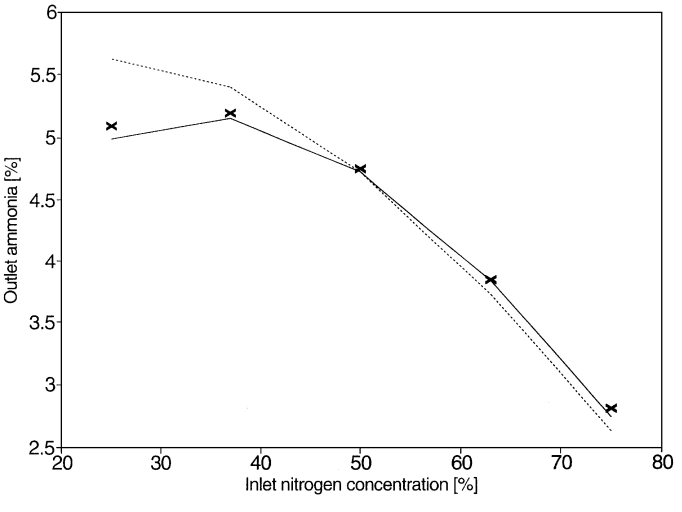

FIG. 5. Percentage of ammonia at outlet versus the inlet gas composition (0% NH_3). Solid line: calculated from Table 4. Dashed line: calculated from Table 1. ×: experimental results. Conditions: 50 atm, 673 K, 0.76 g doubly promoted catalyst (18), sieve size 0.1–0.15 mm, 267 cm^3/min.

6. EFFECTS OF POTASSIUM

Based on nitrogen TPD and TPA results it was previously concluded that N−∗ is destabilized in the presence of potassium (18, 21). The difference between the N_2 desorption equilibrium isobars in Fig. 4 supports this interpretation.

The "bump" (e in Fig. 9) in the TPA profile just before desorption is missing or weak for the singly promoted samples. This raises the following question: Does the adsorption zone corresponding to the first TPD peak move up in temperature when potassium is added? This means that it coincides with the main dip for the potassium-free samples, while it shows up as the bump in the potassium-promoted catalysts. As described in Ref. (18), the identification of a correspondence between the different TPD peaks and adsorption zones is difficult. More experiments, probably of another type, are necessary to clarify whether the sites corresponding to the first TPD peak adsorb nitrogen at a higher temperature for the potassium-promoted sample. To put it another way, is the activation energy for dissociation of N_2 really lower for samples without potassium? This is not what would be expected from single-crystal studies (33, 34), but the idea is consistent with the suggested decrease in the heat of chemisorption of nitrogen, since an increase in the height of the barrier of the dissociation step would be as expected from simple considerations based on Lennard–Jones diagrams. The results in Ref. (13) could actually also be interpreted that way; however, a closer inspection of the TPA profiles reveals features that can be interpreted both ways as a matter of taste.

Figure 6 shows the calculated TPA profiles for activation energies of desorption of N_2 of 146 and 163 kJ mol^{-1} corresponding to samples with and without potassium, respectively. The activation energy for adsorption has also been varied, from 57.6 to 52 kJ mol^{-1} for the desorption energy corresponding to potassium-free samples. The result for this case is the solid line in Fig. 6. The similarity with the experimental results for a singly promoted sample (18) is high for the high-temperature adsorption zones (d and e).

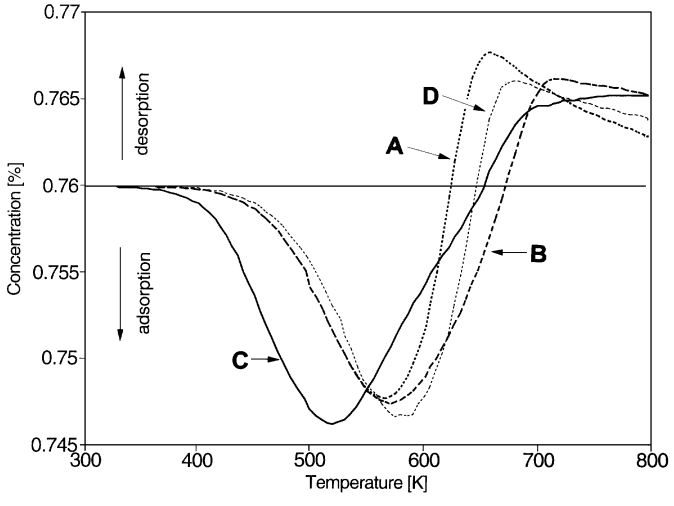

FIG. 6. Calculated TPA profiles (see Table 6 for definitions and Table 4 for preexponential factors). Number of active sites: 1.2×10^{19}. The horizontal thin line indicates the nitrogen concentration at the inlet. A and B coincide below 550 K.

It was suggested a long time ago (35) that the promoting effect of potassium could be caused by a destabilization of the hydrogenated species, NH_x. Obviously, this will lead to increased activity if the coverage of these species is nonnegligible. Starting from the parameters in Table 1 it turned out to be impossible to obtain an appropriate size of the effect, while maintaining the activity, the synthesis activation energy, and the reaction orders at approximately the correct values.[1] The reason is that the calculated amount of NH_x on the surface is small for the parameters in Table 1. As demonstrated below, this situation is significantly changed for the model based on studies of chemisorption on catalysts.

It is frequently claimed that there is no effect of potassium on the activity at 1 atm. This claim is not quite in agreement with our results. Generally, we find an increase in activity by about a factor of 2, while the effect is an order of magnitude at 100 atm (18). Table 5 demonstrates that the destabilization of N−∗ results in a substantial increase in the activity at 1 atm and a 40% higher relative increase at 100 atm (Table 5A, columns 1–3). For the same change in activity at 100 atm, the destabilization of NH−∗ has a relatively weaker effect at 1 atm (Table 5B, columns 5 and 6). In addition, it is conceivable that the activity of the potassium-free sample contains a significant contribution from the sites corresponding to the second or even third peak in the TPD profile. This leaves us with ample opportunities to fit the kinetic experiments for both types of catalyst; however, from a fundamental point of view, this is not a very sound approach as long as the coverage dependences have not been taken properly into account. Much can be said for and against the various explanations. For instance, it would be expected that the destabilization of NH−∗ would lead to an increase in the activation energy for hydrogenation of N−∗, contrary to the experimental observation that the formation of NH_3 during the temperature-programmed surface reaction (TPSR) of N−∗ in H_2 sets in at a lower temperature for the potassium-promoted samples (27). Thus, it is obvious that an exact picture requires further studies of the elementary reaction steps at surfaces with and without potassium and, probably, also additional studies of the

[1] Recently, these calculations were repeated by Stoltze and Nørskov (26); however, these authors were concerned only about the relative variation with pressure of the activities of samples with and without potassium, and they did not seem to realize the extent of these problems.

TABLE 5

Calculations for 50% Conversion[a]

(**A**)							
E_a step 0		57.6	57.6	57.6	40.9	40.9	74.3
E_d step 0		146.3	163.0	163.0	163.0	146.3	146.3
E_a rev. step 3		20.9	12.5	20.9	20.9	20.9	20.9
Q		88.7	105.4	105.4	122.1	105.4	72.0
P (atm)	T (K)						
100	633	85	5	5	5	118	72
100	673	318	22	23	24	439	116
1	673	116	11	11	14	218	24
E_a (syn)		54	59	59	57	42	86
(**B**)							
E_a rev. step 3		20.9	37.6	46.0	54.3	58.5	62.7
P (atm)	T (K)						
100	633	85	78	57	19	7	2
100	673	320	294	210	78	32	10
1	673	116	115	110	97	82	59
E_a (syn)		54	52	51	55	61	69

[a] First four rows: chosen energies, i.e., activation energies of adsorption (E_a) and desorption (E_d) and heat of chemisorption (Q). Next three rows: calculated forward rates of reactions in units of 10^4 s^{-1} for the indicated pressure and temperature. Last row: activation energy of synthesis (E_a) for 100 atm and 673 K. All energy units: kJ mol^{-1}. In Table 5B, Q and the activation energies for step 0 have been omitted since they are constant (values as in the first column of Table 5A).

mutual interaction of the reaction intermediates. It should be noted that the coverage of NH_3–* predicted by all the microkinetic models published so far is negligible. They are all dealing only with sites of metallic character, so the suggested effect of NH_3–* adsorbed on acid sites on the alumina (31) is outside the scope of this paper.

7. COVERAGE-DEPENDENT RATE CONSTANTS

No coverage dependences of the rate constants were taken into account above, to simplify the kinetic model. It would not be consistent to elaborate on the influence of the coverage of one species on the rate constants while ignoring that possibility for the others. In addition, it is not at all clear how any mutual interaction between the various species could affect the results.

Recent results of analysis of N_2 TPD profiles for a Topsøe KM1 catalyst (28) suggest an increase in the activation energy of adsorption of 30 kJ mol^{-1} on going from zero to full coverage; however, in Ref. (28) the rate of adsorption was not measured, and the data analysis was performed *assuming* that the rate of readsorption was significant at low coverage, as follows from the data in Table 1. The results in Ref. (18) suggest otherwise, and a variation of about 13 kJ mol^{-1} for the activation energy of desorption is consistent with the present data as demonstrated below.

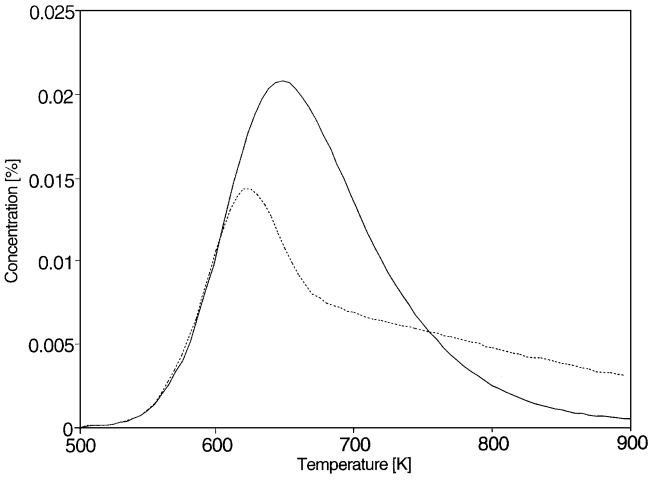

FIG. 7. Effect of coverage dependence on calculated TPD profiles. Rate constants from Table 6. Number of active sites: 1.5×10^{19}. Solid line: TPD in helium. Dashed line: TPD in 0.76% N_2 in helium. This curve has been displaced by 0.76% in the vertical direction.

Figure 7 shows the results of calculation of TPD profiles, where the activation energy for associative desorption (Table 6) has been assumed to vary with coverage in the following way:

$$E_d = (146.3 + 12.5 \cdot \theta_{N-*})\ \text{kJ mol}^{-1}. \qquad [9]$$

The agreement for the "normal" TPD (in helium) and TPD in a dilute N_2/He mixture (Fig. 8) is good, even though the left side of the experimental normal TPD peak is slightly wider than for the calculated profile. It should be emphasized that the rather weak effect of the presence of 0.76% N_2 in the inlet gas stream demonstrates that the effect of readsorption under the normal TPD conditions ($\leq$0.03% N_2) is negligible and, in addition, that the experimental results are strongly in disagreement with the equilibrium constant for the nitrogen chemisorption which can be deduced from the Stoltze–Nørskov model, as already suggested in the discussion of Fig. 2. The deviation arises from an uncritical use by Stoltze and Nørskov of the high heat of chemisorption for nitrogen (169 kJ mol^{-1}) determined for zero coverage.

TABLE 6

Activation Energies for Step 0 Used in the Calculation of the TPA Profiles in Figs. 6, 7, and 9

Activation energy (kJ mol^{-1})		Figure and label
Adsorption	Desorption	
57.60	146.3	6A, 9A
57.60	163.0	6B
52.04	163.0	6C
57.60	$146.3 + 12.54 \cdot \theta_{N-*}$	7D, 9D

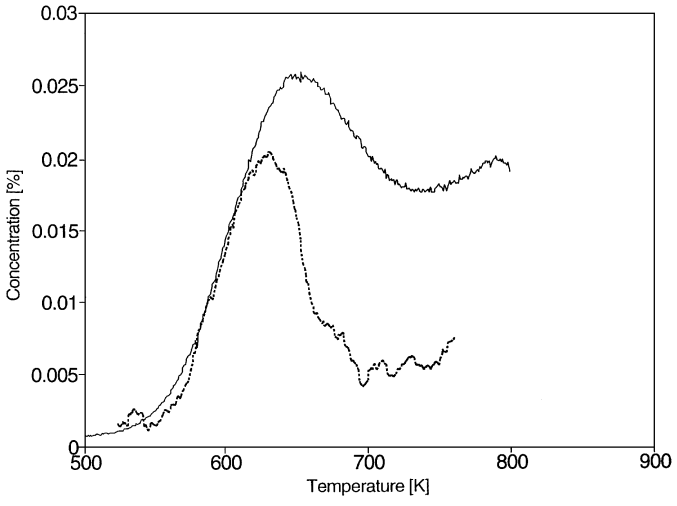

FIG. 8. Experimental TPD results for multiply promoted sample. Solid line: TPD in helium. Dashed line: TPD in 0.76% N_2 in helium. This curve has been displaced by 0.76% in the vertical direction.

The calculations show that even for the modified Stoltze–Nørskov model (26), readsorption effects will cause a shift of the peak to a temperature higher than 900 K in the presence of 0.76% N_2.

The result of a calculation of the TPA profile using Eq. [9] is shown in Fig. 9. The desorption zone above 650 K has become more flat, in agreement with the experimental results. It is, of course, unlikely that E_{ad} is constant when E_d varies, but the presented calculation is meant only as an example of the possible effects of variations in the rate constants with coverage. Such effects are most easily described by variations in one of the activation energies; in the present case quite small variations will suffice. It can be argued that the preexponential factor should be varied as well, but the available data do not justify more complicated modeling.

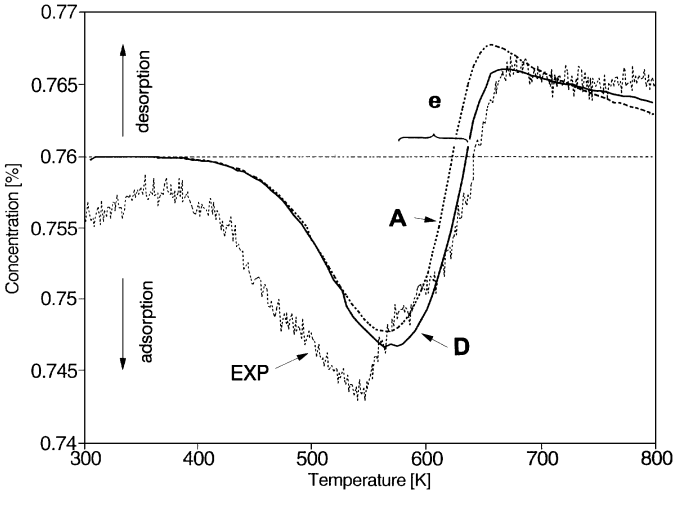

FIG. 9. Effect of coverage dependence on the TPA profiles (solid line, D). Rate constants from Table 6, A and D. Number of active sites: 1.2×10^{19}. (A) No coverage dependence, for comparison. EXP: experimental results for doubly promoted sample. e = the "bump."

8. DISCUSSION

The case history discussed above clearly demonstrates the familiar experience with kinetic modeling that there is more than one way of obtaining a good fit to a set of experimental data; the models defined by Eqs. [0] to [7] and Table 2 (column II) or 4 both result in fairly good fits to the data in Fig. 1. The inevitable conclusion is that a kinetic model should be judged by a sound set of criteria, not just by the fit to some set of experimental synthesis data, even when it represents a rather extended excursion in the parameter space. In particular, one should not rely on the "45° plots." A detailed check of the activation energy and the reaction orders should be made. We suggest the following list of criteria that the model should satisfy:

1. The rate-determining step should be (a) correctly chosen and (b) reasonably described (order of magnitude and temperature dependence correct over the relevant experimental range).
2. The fraction of empty sites and the coverages of the most important reaction intermediates should be reasonably correct (as estimated by independent methods).
3. The derived kinetic equation should fit synthesis data over a wide range of conditions.

The importance of these criteria depends on the aim of the study of the kinetics. If the aim is to obtain an accurate description of the process, then criterion 3 is the most relevant. Criteria 1 and 2 are the most important when fundamental insight is the major purpose of the study.

Concerning criterion 3 above, a perfect 45° plot is a necessary but not sufficient condition. Any visibly deviating trend should be taken as a very serious indication that something may be fundamentally wrong. If the 45° plot is perfect, the model should still be checked for systematically deviating trends in the rate-versus-temperature or rate-versus-partial pressure plots, as in Fig. 5, before it is finally evaluated. In other words, the 45° plots cannot be used to demonstrate that a model is good, only that it is poor. The model based on Table 1 fails to satisfy this condition.

An evaluation of criterion 1b results in rejection of the input parameters in Tables 1 and 2. They cannot reproduce the nitrogen chemisorption results for the catalysts in question. This leaves us with Table 4, which is not in direct contradiction with any published data for fused iron oxide ammonia synthesis catalysts, considering the simplifying assumptions behind the model. Criterion 2 is difficult to evaluate since only very few attempts to measure the coverages

directly have been published (36). A relative estimate of the N−∗/H−∗ balance is indicated by Fig. 5, and at least we can claim that the model is self-consistent, since the calculated coverages of N−∗ and H−∗ under synthesis conditions are close to 0.5 (21), which was the coverage used in the determination of the rate constants; however, the calculated activation energy of ammonia synthesis varies from 110 to 43 kJ mol^{-1} for conversions from 0 to 100% at 100 atm and 673 K. Such a large variation is not observed experimentally. The experimental reaction order in NH_3 is also more constant and less negative (ca. −1.5, as described by the Pyzhev–Temkin models) than calculated for high conversion from Langmuir models (−2) (1, 2, 22, 23). This suggests that it is necessary to take coverage dependences arising from intrinsic surface heterogeneity or from adsorbate–adsorbate interactions into account, as indeed was concluded half a century ago. The same conclusion can be drawn from N_2 or H_2 TPD, N_2 TPA, or TPSR of N−∗ in H_2. It has recently been suggested that Bragg–Williams or quasi-chemical isotherms might provide a better basis for a kinetic analysis of the surface reactions on iron NH_3 synthesis catalysts (2).

The best way to determine the relevant input parameters for a microkinetic model of a synthesis reaction over a catalyst is from surface reaction studies of the very same catalyst, whenever possible. This approach has the advantage that it is not necessary to rely on any assumptions about the dominance of a particular crystal plane, and it is probably much faster than single-crystal studies, since for the present case both N_2 TPD and TPA, H_2 TPD, TPSR, and isobars (adsorption or desorption) can be quickly measured.

9. CONCLUSIONS

A model for ammonia synthesis has been obtained that is fairly consistent with the rates of nitrogen chemisorption as well as ammonia synthesis over a wide range of experimental conditions. It is probably as close as one can reasonably expect to get within the Langmuir approximation; however, the extended Temkin models are still superior (2).

It has been demonstrated that it is possible to obtain a good "45° fit" between a Langmuir type of microkinetic model and ammonia synthesis data for iron-based catalysts, for both positive and negative activation energies for the dissociation of nitrogen. This accentuates the need for independent estimates of the critical input parameters.

The microkinetic analysis based on the surface reaction studies of catalysts displays much better agreement with experimental data for the ammonia synthesis reaction than similar models based on single-crystal data. In addition, an inconsistency between these models and experimental nitrogen TPD results for the catalysts is demonstrated.

The destabilization of N−∗ by potassium results in a significant increase in the calculated activity. A similar effect can be obtained by destabilization of NH−∗. The two effects differ in the way that for the same relative change in pressure dependence, the order of magnitude of the activity is most strongly affected by the destabilization of N−∗. It is conceivable that both effects are of some importance for the activity of the industrial iron catalyst; however, the TPSR results (27) suggest that the destabilization of N−∗ is the most important factor.

ACKNOWLEDGMENTS

The author expresses special thanks to Susanne Lund Andersen for sharing her great experience and giving instructions on the true magnitude of the activation energy of ammonia synthesis. In addition, the author has benefitted from discussions with J. Dumesic, H. Topsøe, M. Muhler, I. Alstrup, J. Bøgild Hansen, E. Törnqvist, B. Clausen, and J. Nørskov, and is grateful to J. Dumesic, L. Aparicio, and A. Treviño for making available their kinetic analysis computer programs.

REFERENCES

1. Bøgild Hansen, J., *in* "Ammonia, Catalysis and Manufacture" (A. Nielsen, Ed.). Springer-Verlag, Berlin, 1995.
2. Aparicio, L. M., and Dumesic, J. A., *Top. Catal.* **1**, 233 (1994).
3. Bowker, M., Parker, I. B., and Waugh, K. C., *Appl. Catal.* **14**, 101 (1985).
4. Stoltze, P., and Nørskov, J. K., *Phys. Rev. Lett.* **55**, 2502 (1985).
5. Stoltze, P., and Nørskov, J. K., *J. Vac. Sci. Technol. A* **5**, 581 (1987).
6. Stoltze, P., *Phys. Scr.* **36**, 824 (1987).
7. Parker, I. B., Waugh, K. C., and Bowker, M., *J. Catal.* **114**, 457 (1988).
8. Bowker, M., Parker, I. B., and Waugh, K. C., *Surf. Sci.* **197**, L223 (1988).
9. Stoltze, P., and Nørskov, J. K., *Surf. Sci.* **197**, L230 (1988).
10. Stoltze, P., and Nørskov, J. K., *J. Catal.* **110**, 1 (1988).
11. Dumesic, J. A., and Treviño, A. A., *J. Catal.* **116**, 119 (1989).
12. Geus, J. W., and Waugh, K. C., *in* "Catalytic Ammonia Synthesis, Fundamentals and Practice" (J. R. Jennings, Ed.), p. 179. Plenum, New York, 1991.
13. Emmett, P. H., and Brunauer, S., *J. Am. Chem. Soc.* **56**, 35 (1934).
14. Scholten, J. J. F., Zwietering, P., Konvalinka, J. A., and de Boer, J. H., *Trans. Faraday Soc.* **55**, 2166 (1959).
15. Paál, Z., Ertl, G., and Lee, S. B., *Appl. Surf. Sci.* **8**, 231 (1981).
16. Rettner, C. T., and Stein, H., *J. Chem. Phys.* **87**, 770 (1987); *Phys. Rev. Lett.* **59**, 2768 (1987).
17. Bowker, M., *Catal. Today* **12**, 153 (1992).
18. Fastrup, B., *J. Catal.* **150**, 345 (1994).
19. Dumesic, J. A., Rudd, D. F., Aparicio, L. M., Rekoske, J. E., and Treviño, A. A., "The Microkinetics of Heterogeneous Catalysis." Am. Chem. Soc., Washington, DC, 1993.
20. Seebauer, E. G., Kong, A. C. F., and Schmidt, L. D., *Surf. Sci.* **193**, 417 (1988).
21. Fastrup, B., *Top. Catal.* **1**, 273 (1994).
22. Nielsen, A., "An Investigation on Promoted Iron Catalysts for Ammonia Synthesis," 3rd ed. Gjellerup, Copenhagen, 1968.
23. Nielsen, A., Kjær, J., and Hansen, B., *J. Catal.* **3**, 68 (1964).
24. Ertl, G., Lee, S. B., and Weiss, M., *Surf. Sci.* **114**, 515 (1982).
25. Waugh, K. C., Butler, D. A., and Hayden, B. E., *Top. Catal.* **1**, 43, 295 (1994).
26. Stoltze, P., and Nørskov, J. K., *Top. Catal.* **1**, 253 (1994).
27. Fastrup, B., Muhler, M., Nygård Nielsen, H., and Pleth Nielsen, L., *J. Catal.* **142**, 135 (1993).
28. Muhler, M., Rosowski, F., and Ertl, G., *Catal. Lett.* **24**, 17 (1994).

29. Boudart, M., and Djéga-Mariadassou, G., "Kinetics of Heterogeneous Catalytic Reactions." Princeton Univ. Press, Princeton, NJ, 1984.
30. Waugh, K. C., "Elementary Reaction Steps in Heterogeneous Catalysis" (R. W. Joyner and R. A. van Santen, Eds.), NATO ASI Series C: Mathematical and Physical Sciences, Vol. 398, p. 419. Kluwer Academic, Bordrecht/Norwell, MA, 1993.
31. Frankenburg, W. G., "Catalysis," Vol. III, Ch. 6, p. 171. Reinhold, New York, 1955.
32. Topsøe, H., Topsøe, N., Bohlbro, H., and Dumesic, J. A., *in* "Proceedings, 7th International Congress on Catalysis, Tokyo, 1980" (T. Seiyama and K. Tanabe, Eds.), p. 247. Elsevier, Amsterdam, 1981.
33. Ertl, G., Lee, S. B., and Weiss, M., *Surf. Sci.* **114**, 527 (1982).
34. Ertl, G., Weiss, M., and Lee, S. B., *Chem. Phys. Lett.* **60**, 391 (1979).
35. Love, K., and Emmett, P. H., *J. Am. Chem. Soc.* **63**, 3297 (1941).
36. Nwalor, J. U., Goodwin, J. G., and Biloen, P., *J. Catal.* **117**, 121 (1989).